

PHOTODISINTEGRATION OF He^3 [†]

B. L. Berman, L. J. Koester, Jr., and J. H. Smith

University of Illinois, Urbana, Illinois

(Received 5 April 1963)

The 90° differential cross sections for the photodisintegration of He^3 into a proton and a deuteron have been measured for incident photon energies between 8.5 and 22 MeV. The fact that the incident photon momentum is small at these energies provides a unique signature for this process. The proton and deuteron are emitted nearly back to back with equal momenta; hence the energy of the proton is about twice that of the deuteron. In the competing 3-body disintegrations, the angular correlation and relative energy of the two protons are not similarly fixed by kinematics.

The 22-MeV bremsstrahlung beam from the betatron was collimated through a four-foot shielding wall. At the position of the target, the beam was 2 cm square. The incident flux was measured by an NBS-type¹ Dural ionization chamber located 6.5 m beyond the target.

The He^3 target chamber (Fig. 1) was constructed of brass, with thin Alumiseal windows for the x-ray beam. This chamber was filled with He^3 gas at slightly less than atmospheric pressure. CsI(Tl) crystals, 2.85 cm square and 1 mm thick, were mounted symmetrically inside the chamber 5 cm from the beam axis (Fig. 1). The conical Lucite light pipes also served as gas-tight windows, and were silvered on all surfaces except where they were in contact with the crystals and phototubes. An evaporated layer of aluminum on the surface of each crystal completed the reflecting enclosure.

Fast coincidences between the anode signals of the two counters were used to trigger a Tektronix-551 dual-beam oscilloscope. The dynode pulses were integrated with an RC time constant of 1 μsec , amplified linearly, displayed on the oscilloscope,

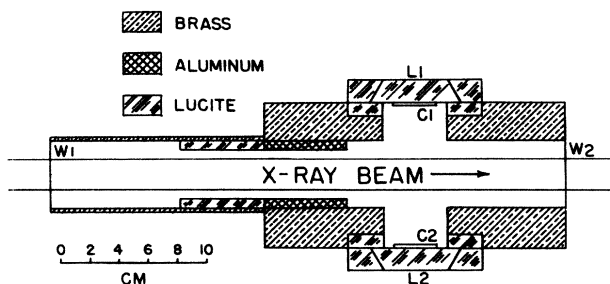


FIG. 1. He^3 target chamber. C1 and C2 are CsI(Tl) crystals, L1 and L2 are light pipes, and W1 and W2 are thin Alumiseal windows. Gaskets and flanges are omitted for clarity.

and photographed. Since all the particles were stopped in the crystals, their energies were determined by pulse-height measurement. Electrons were rejected by comparing the pulse amplitude at 3.5 μsec with the peak height, since the fluorescent decay time constant of CsI(Tl) varies with particle velocity.^{2,3} The nearly linear gain of the preamplifiers and oscilloscope was calibrated with a mercury switch pulser. Figure 2 shows the resulting correlated pulse heights from a pair of counters.

Of 26120 photographs analyzed, 4432 consist of pairs of heavy particles. Half of these appear on Fig. 2, where the clustering of points around the two-to-one pulse-height ratio characteristic of two-body disintegration is readily apparent. In order to double the effective counting rate, a second pair of counters was mounted at right angles to the first. It gave results in all ways consistent with those of Fig. 2 within expected statistical fluctuations.

The spread in the $p-d$ points is caused by (i) the

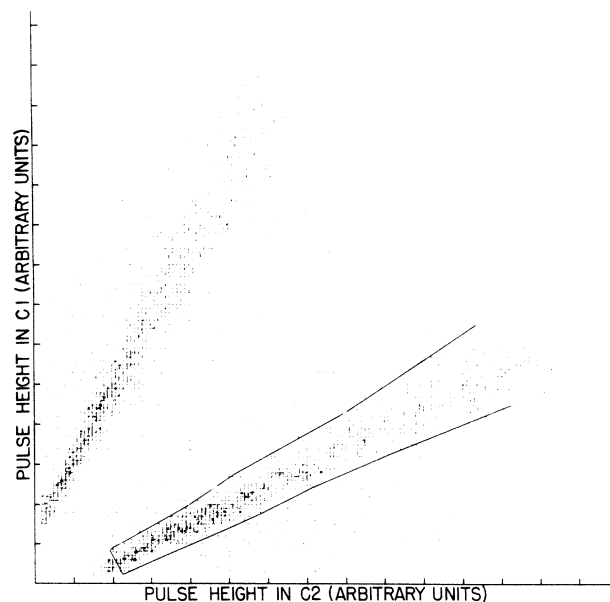


FIG. 2. Data points from counters C1 and C2. Points in the densely populated areas are $p-d$ coincidences from $\text{He}^3(\gamma, p)d$. The solid lines are drawn on the lower branch to show our boundaries for excluding scattered $p-p$ coincidences from $\text{He}^3(\gamma, 2p)n$ (see text) and the cutoff at 8.5-MeV incident photon energy.

kinematical spread associated with the finite beam width and the angular interval subtended by the counters; (ii) the spread in energy loss of the charged particles owing to the varying path lengths of gas traversed; and (iii) the instrumental resolution. Limits calculated on the basis of (i) and (ii) above contain about 85% of the accepted events; the limits actually used were chosen to coincide with the abrupt change in density of the data points (see Fig. 2). The error in either direction introduced by this procedure is compensated to a high degree by the method of subtraction of the background of $p-p$ coincidences from the three-body disintegration.

There are 3824 events which satisfy the criteria for two-body disintegration with incident photon energy above 8.5 MeV, and 422 events which are considered to be $p-p$ coincidences. We measured the density of these $p-p$ coincidences on Fig. 2 and, assuming a smooth variation with position, subtracted the number which would be indistinguishable from $p-d$ events. This number was never larger than 9.5% at any energy and averaged 7.6%.

The arbitrary pulse-height scale of Fig. 2 was calibrated in energy units by fitting the data to the high-energy cutoff of the bremsstrahlung spectrum. This calibration took account of the energy losses in the He^3 gas and aluminum crystal coating, and the variation in scintillator efficiency with the specific ionization of the incident charged particle.⁴

The photon energy which produced each event is the sum of the proton and deuteron energies plus 5.49 MeV. Thus the number of events falling in a 1-MeV interval of photon energies is divided by the corresponding number of photons in the bremsstrahlung spectrum.⁵ The target volume effective in producing coincidences and the effective solid angle of the counters were calculated geometrically. Figure 3 shows the resulting cross sections with purely statistical errors indicated. To these should be added systematic errors of up to 5%.

Total cross sections for the two-body photodisintegration have been calculated by several authors.⁶⁻⁸ To compare with our differential cross sections, we multiply their results by $3/8\pi$ corresponding to a $\sin^2\theta$ angular distribution.⁹ Our data do not agree with cross sections based on Gaussian^{6,7} or pure exponential⁸ wave functions for He^3 . When the size parameter is adjusted to bring the peak to 11 MeV, the cross section becomes much too large. With Irving's

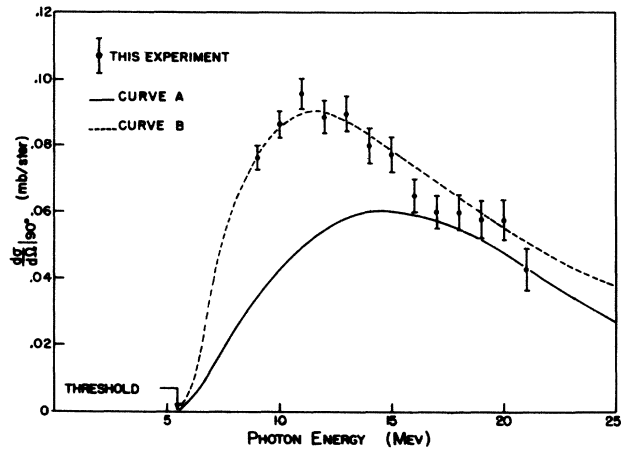


FIG. 3. The 90° differential cross sections for the $\text{He}^3(\gamma, p)d$ photodisintegration. Curve A is taken from reference 6. Curve B is computed from reference 7. No normalization has been performed.

wave function of the form⁷

$$\Psi_{\text{He}} = A \exp[-\mu(\sum_{i>j} r_{ij}^2)^{1/2}] / (\sum_{i>j} r_{ij}^2)^{1/2}, \quad (1)$$

where r_{ij} is the distance between nucleons i and j , and the size parameter $1/\mu = 2.6 \text{ F}$, a good fit to our data is obtained (dashed curve in Fig. 3). A 5% change in $1/\mu$ spoils the fit noticeably.

The rms nuclear radius computed with this wave function (1) is $\langle r^2 \rangle_{\text{He}}^{1/2} = 1.9 \text{ F}$. The rms charge radius, according to

$$\langle r_{\text{charge}}^2 \rangle_{\text{He}} = \langle r^2 \rangle_{\text{He}} + \langle r_{\text{charge}}^2 \rangle_{\text{proton}}$$

is $\langle r_{\text{charge}}^2 \rangle_{\text{He}} = 2.0 \text{ F}$, in agreement with electron-scattering measurements of Collard and Hofstadter.¹⁰ The wave function (1) was also used to calculate the He^3 nuclear form factor, which was then multiplied by¹¹ $F_{\text{charge proton}}$ to compare with the He^3 charge form factor measured by electron scattering.¹⁰ Our calculated form factor becomes larger than the measured one by about 20% only at the larger values of momentum transfer squared q^2 approaching 5 F^{-2} .

The photodisintegration cross section apparently is very sensitive to nuclear size. We feel that a theoretical treatment correlating these results with the electron-scattering data would be most valuable.

The cooperation of the betatron engineers and staff is gratefully acknowledged. Eugene Beier, John O'Fallon, and Nanch O'Fallon assisted in taking and processing the data. We wish to thank

Professor D. G. Ravenhall for several valuable discussions.

[†]Work supported in part by the U. S. Office of Naval Research.

¹J. S. Pruitt and S. R. Domen, National Bureau of Standards Report No. 6218, 1958 (unpublished).

²R. S. Storey, W. Jack, and A. Ward, Proc. Phys. Soc. (London) **72**, 1 (1958).

³J. C. Robertson and J. G. Lynch, Proc. Phys. Soc. (London) **77**, 751 (1961).

⁴R. B. Murray and A. Meyer, Phys. Rev. **122**, 815 (1961).

⁵A. S. Penfold and J. E. Leiss, University of Illinois

Physics Research Laboratory Report, 1958 (unpublished).

⁶M. Verde, Helv. Phys. Acta **23**, 453 (1950).

⁷J. C. Gunn and J. Irving, Phil. Mag. **42**, 1353 (1951).

⁸C. Rossetti, Nuovo Cimento **14**, 1171 (1959).

⁹We wish to thank Dr. Cranberg for sending us his data, which indicate a strong $\sin^2\theta$ contribution: $0.37 + (1 + 0.8 \cos\theta) \sin^2\theta$. See L. Cranberg, Bull. Am. Phys. Soc. **3**, 173 (1958).

¹⁰We thank Professor R. Hofstadter for communicating these results prior to publication.

¹¹ F charge is defined by Eq. (A-23) in D. R. Yennie, M. M. Levy, and D. G. Ravenhall, Rev. Mod. Phys. **29**, 144 (1957). Experimental values for the proton were taken from F. Bumiller, M. Croissiaux, E. Dally, and R. Hofstadter, Phys. Rev. **124**, 1623 (1961).

$(p, 2p)$ ANGULAR CORRELATIONS IN THE DISTORTED-WAVE BORN APPROXIMATION*

K. L. Lim[†] and I. E. McCarthy[‡]

Department of Mathematical Physics, University of Adelaide, Adelaide, South Australia

(Received 6 May 1963)

The angular correlation in a $(p, 2p)$ experiment involving a proton in a definite shell-model state contains information about both the shell-model state and the distortion of the wave functions of the unbound particles in the entrance and exit channels.¹ In order to see what information can be reliably identified, it is necessary to do a distorted-wave Born-approximation calculation. Previous calculations² of angular correlations have used plane waves modified by space weighting factors calculated semiclassically.

A fully distorted-wave calculation of the angular correlation in the case where the momentum vectors of the final-state particles are symmetrical about the incident direction and coplanar with it has been coded for the IBM 7090. The struck proton may be initially in either an s state or a p state. A parameter study on the results of the 155-MeV $C^{12}(p, 2p)B^{11}$ experiment of Garron *et al.*³ is reported here.

The approximations used are as follows:

$$d^3\sigma/d\Omega_L d\Omega_R dE_L = \frac{2\pi m_0}{\hbar} \frac{2m_0^3}{\hbar k_0 (2\pi\hbar)^6} (E_L E_R)^{1/2} \\ \times \sum_{M, M_1, m} C(J_1 j J; M_1 M - M_1)^2 \\ \times C(ls j; m M - M_1 - m)^2 |M_l^m|^2.$$

This formula involves the extreme single-particle model with $j-j$ coupling. J_1 , j , and J are the angular momenta of the residual nucleus, the struck particle, and the initial nucleus; M_1 , m ,

and M are the magnetic quantum numbers; l and s are the orbital angular momentum and spin of the struck particle. m_0 is the proton mass.

$$M_l^m = \iint d^3r_1 d^3r_2 \chi^{(+)}(\vec{k}_0, \vec{r}_1) \chi^{(-)*}(\vec{k}_L, \vec{r}_1) \\ \times \chi^{(-)*}(\vec{k}_R, \vec{r}_2) \psi_l^m(\vec{r}_2) v_{12} \delta(\vec{r}_1 - \vec{r}_2).$$

$\chi^{(+)}$ and $\chi^{(-)*}$ are optical-model wave functions for ingoing and outgoing particles. $\hbar\vec{k}_0$ is the momentum of the incident proton, and $\hbar\vec{k}_L$ and $\hbar\vec{k}_R$ are the momenta of final-state particles scattered to the left and right, respectively. $k_L = k_R$, and they are on opposite sides of the \vec{k}_0 direction at an angle θ . All quantities are in the center-of-mass system. The optical-model parameters used were V_1 , W_1 , R , and a for the initial state and V_2 , W_2 , R , and a for the final state describing Woods-Saxon form factors.

For the shell-model wave function ψ_l^m of the struck proton, we have used finite square-well wave functions treating the radius R_b as a parameter and adjusting the binding energy to be equal to the experimentally observed removal energy, thus neglecting rearrangement energy.

The impulse approximation has been shown² to give the right order of magnitude. We feel that this is all it can do, so we have retained one arbitrary normalizing parameter v_{12} and have not attempted to describe the absolute magnitude of the cross sections. Provision has been made for finite-range interaction, and a more realistic